IIETA International Information and Engineering Technology Association
Advancing the World of Information and Engineering

Journal Européen des Systèmes Automatisés
Vol. 59, No. 3, March, 2026, pp. 631-640
Journal homepage: http://iieta.org/journals/jesa

Application of ARM-Based Integrated Circuits and Wireless Sensor Networks in the Development of a Data-Logging System for Coal and Mineral Plants in Vietnam

Alberto Coboi, Nam Pham Van*, Oraiden Manuel Sabonete

School of Electrical and Electronic Engineering (SEEE), Hanoi University of Industry, Hanoi 100000, Vietnam

Corresponding Author Email: nampv@haui.edu.vn

https://doi.org/10.18280/jesa.590307

Received: 3 November 2025
Revised: 13 January 2026
Accepted: 31 January 2026
Available online: 31 March 2026

Keywords:
Advanced RISC Machine microcontroller, environmental monitoring, Internet of Things, Long Range communication, mining safety, wireless sensor networks

ABSTRACT

The coal mining sector is one of the largest industries in Vietnam and makes a significant contribution to the national economy. Nevertheless, operational safety and efficiency remain challenging because of unstable underground conditions and the limited responsiveness of existing monitoring systems. This paper presents a case study on the design and deployment of a reliable, low-power, and scalable environmental monitoring system for an industrial setting. The proposed system collects temperature, humidity, gas concentration, and light intensity data from two nodes, namely a slave node and a master node, within the monitored area through a Long Range (LoRa)-based wireless sensor network. To satisfy dependability requirements under field conditions with intermittent connectivity, a hybrid architecture is developed in which data can be transmitted to a cloud platform via an ESP8266 Wi-Fi module while also being displayed locally for on-site and offline access. With potential applicability to similar industrial environments, the proposed solution offers a flexible and energy-efficient framework for improving safety and operational management in coal and mineral plants in Vietnam.

1. INTRODUCTION

Coal mining in the underground mines of Vietnam has increased considerably in the last 2 decades, where the coal production growth rate has risen by 5 times between 2000 and 2018 (4.3 million tonnes to 22.1 million tonnes). There are forecasts that the total production of coal will be 41 million tons in 2019, 47.8 million tons in 2020, and 49.3 million tons in 2025, according to the Master Plan of Coal Industry Development in Vietnam in 2020 with a perspective till 2030 [1]. The coal mining industry is now a major contributor to the economic growth of Vietnam, considering the increasing demand for coal in the domestic and international markets. However, the coal mining industry in Vietnam has a number of challenges, which include increased output of coal, prospecting and exploration, technology used in coal mining, environmental concerns, and sustainable development [2].

The safety of the workers at the coal mines is a concern to many miners. Mines in the underground prevent workers' inhalation of heat, dust, and poisonous gases; this may result into sickness, harm, and even demise [3]. Industrial Internet of Things (IIoT) was developed due to the utilization of the Internet of Things (IoT) in industrial systems and other recent technological advancements. The IIoT can help in addressing the inefficiency of the old method of monitoring and controlling where businesses can have one monitoring system to provide automation in the process, provide a secure working environment, effectively enforce rules and regulations, and control environmental issues. Based on the advantages that IoT can offer to the fore, it is quite understandable that most mining companies have invested more in the practice, after introducing IoT-enabled solutions to their organizations to enhance environmental sustainability, productivity, and safety of mining procedures [3, 4].

To eliminate these limitations, the proposed research suggests an IoT-based datalogger system built on the Advanced RISC Machine (ARM) Cortex family that possesses impressive features and is suitable to be developed as an embedded. Also, the embedded system design is possible due to the wireless sensor node. The nodes, based on an ARM Cortex microcontroller, are meant to track the coal mining industry. As a result, low-power sensor nodes with high accuracy are needed in the development of wireless sensor networks. Nodes can be designed using microcontrollers that have promising features. The characteristics of sensor nodes are subject to hardware and software design problems [5]. Long Range (LoRa) forms the physical layer and the long-distance connection, whereas the communication protocol and network system model are established by the LoRaWAN architecture, which is known as a star of stars. This protocol affects the battery life of a node, the network capacity, QoS, security and the number of applications that the network supports. The proposed technology aims at providing a reliable, scalable and affordable data-logging platform that can be customized to fit the coal and mineral plants in Vietnam with a combination of these technologies [6]. IoT is a huge prospect of creating powerful industrial systems and applications by utilizing the rising prevalence of wireless, mobile, and sensor devices along with the radio-frequency identification (RFID). Over the past few years, numerous

industrial IoT applications have been built and put in operation. LoRa, Sigfox, and NB-IoT are a few examples of technologies that are examples of Low-Power Wide-Area Network (LPWAN). These technologies enable long-distance communications in low-power devices at a low cost of operation, which render the same as viable as wireless communication protocols in battery-powered IoT devices [7]. There are a number of review papers that investigate the LPWAN technology as an aspect of the IoT in various ways. Nevertheless, little research has been done to address the role of these technologies in use in different IoT applications [8]. The transfer of data is dependent on the wired and wireless technologies with their own benefits. Ethernet and fiber optic wired systems are fast and secure in a stable environment but have mobility issues. Wireless technologies, i.e., Wi-Fi and 5G, can serve mobile devices and IoT, which is flexible, but with the risk of interference. The technology is determined by the cost, mobility, and performance requirements [9]. The coal and mineral plants in Vietnam are limited by the difficult terrain, deep mining as well as exposure to explosive gases (Vinacomin 2019). The operators should have solutions that can be deployed without being costly. Although there has been increased wireless technology, the coal industry in Vietnam is yet to have efficient data recording systems. Even though Wi-Fi, LoRa, and Zigbee can use low-energy alternatives, cellular networks must be considered with priority because they are scalable and long-range and can fulfill the needs of the industry.

Vinacomin gives much importance to occupational safety and risk management [10]. Due to lack of mechanization, the mining industry in Vietnam is very reliant on artisans, and the mining sector requires specific risk management via training and technology [11]. This paper points out that an efficient system that incorporates both ARM and LoRaWAM technologies is necessary and provides a balance between low-energy consumption and a high rate of performance. Our project is a microcontroller-based, long-range communication system based on the LoRa technology, which is known to be characterized by low power transmissions and a wide range. This system is capable of monitoring the industrial environment in Vietnam in real-time and ensuring that there is good communication. The research will produce a better system design that takes into consideration the issues of the Vietnamese industry. The rest of this paper will be structured in the following way: The Introduction will address the coal industry and monitoring protocol requirements in Vietnam. The problem statement declares the existing constraints of monitoring in adverse conditions. The solution section details the ARM-based STM32 microcontrollers and LoRa wireless communication architecture. The design of the hardware and software will comprise sensor integration, information flow and cloud connectivity through ESP8266 Wi-Fi. Table 1 delineates the various layers within the IoT This paper will provide the testing procedure and experimental outcomes of real-time data collection, and finally suggest the findings and recommendations.

2. SYSTEM ARCHITECTURE

The proposed environmental monitoring system comprises distributed sensor nodes, a communication gateway, and a cloud-based monitoring platform. Figure 1 demonstrates the general system architecture.

Every sensor node will be tasked with the responsibility of monitoring the environment and sending the information wirelessly over the LoRa communication technology. The gathered information is sent to a gateway node that receives the information and sends it to a cloud server via a Wi-Fi connection. The cloud system allows environmental data to be monitored and viewed remotely.

Table 1. Comparison with existing systems

Study	Technology	Parameters	Communication
Reddy et al. [12]	IoT	Temp, Humidity	LoRa
Chowdhury et al. [13]	IoT	Gas monitoring	LoRa
Yadav et al. [14]	WSN	Environmental monitoring	ZigBee
Proposed system	ARM-IoT	Temp, humidity, gas, light	LoRa

There are three key components of the system architecture:

- ✓ Sensor Nodes
- ✓ Gateway Node
- ✓ Cloud Monitoring Platform

The sensor nodes are placed in various places in the mining environment so that the environmental parameters are always measured. Figure 1 indicates the general structure of the proposed environmental monitoring system.

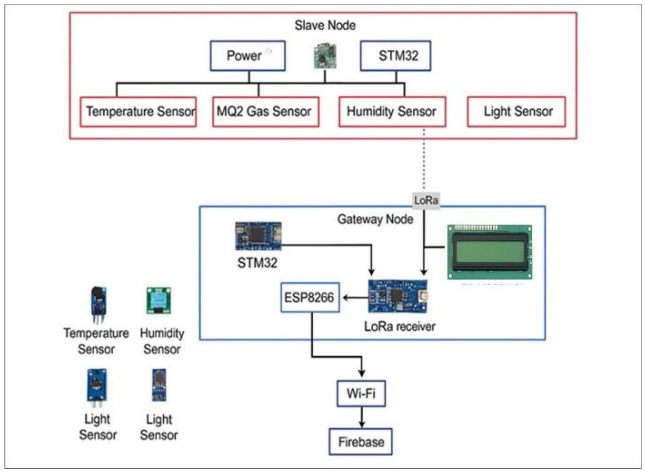

Figure 1. Overall system architecture of the proposed monitoring system

2.1 Problem formulation

The coal and mineral industry is an important aspect of the Vietnamese economy that employs thousands of people and contributes a significant amount to the GDP. The industry, however, has significant challenges of operations, particularly those related to ensuring equipment reliability and employee safety in the hostile conditions that are characterized by dust, high humidity, mechanical vibration and explosive gases. Wired or short-range wireless-based conventional monitoring systems are often costly, inflexible, and would easily fail in such environments. It is difficult to respond promptly to accidents (such as gas leakage or malfunction) due to the fact that these systems do not provide the possibility of remote accessibility and real-time data.

The existing wireless technologies, such as Wi-Fi and Zigbee, cannot be used in large-scale industrial applications

since they are short-range, or consume too much energy. Even though the cellular network has a wide coverage radius, it is costly to maintain and may not provide reliable connectivity in remote and underground locations. Besides, many of the current systems cannot store the data on their own but refer fully to the cloud-based solutions, and in such areas with poor network availability, they will fail to perform their functions. In Vietnamese coal and mineral facilities, such technological gap has led to poor operations, high level of safety risks and high maintenance costs.

2.2 Key challenges

The old systems of monitoring do not help the situation because such systems cannot detect crisis immediately and this causes life-threatening delays in responding to equipment failure or gas leakage. Besides exposing workers to hazards, late detection of hazards incurs costly operations and machinery destruction. The second major disadvantage of this industry is that it uses wire monitoring. These systems are not very flexible in dynamic mining conditions and are demanding in magnitude of physical infrastructure, which makes them more costly to install. The lack of remote monitoring also prevents supervisors to constantly check the status of equipment or environmental conditions in large mining operations due to the absence of remote monitoring. Other wireless solutions like Wi-Fi and Zigbee have been experimented with by numerous operations but these technologies are not reliable and the range is limited in the wide-scale industrial scenarios. The cellular networks have a larger coverage but they cannot be practiced because they are expensive to operate and non-reliable in remote or underground areas. Moreover, the existing systems lack on-site data storage, and thus cannot be useful in some regions where Internet connectivity is poor, and it is a widespread issue in the mining regions of Vietnam.

2.3 Proposed solution

We are proposing a smart industrial monitoring system that will combine sensors with a dynamic communication system. The system has environmental sensors to detect the level of temperature, humidity, flammable gases and intensity of light to monitor the mining conditions in real-time. These sensors are interconnected in distributed ARM microcontroller-based nodes, which are selected due to processing power and energy efficiency. The system relies on the LoRa technology, based on reliable long-range communication and excellent obstacle penetration and low-energy consumption. The dual-layer architecture also guarantees continuous functionality with a local gateway node that interprets the sensor data and sends the data to a cloud storage via Wi-Fi, where accessible and shows the information through Liquid Crystal Display (LCD) interface. This method caches information in the neighbourhood when there is a failure of Internet connections until connectivity is re-established. The system can be used in both large and small mining activities of coal and other minerals. Through this monitoring network, the Vietnamese mining activities can be improved in terms of safety supervision, efficiency and cost-effectiveness hence making the industry become a prototype of the modern monitoring. In this section, the discussion and research findings are explained. The findings may be provided in figures, graphs, tables, and formats so that they can be easily understood by the reader [11, 15]. It is possible to divide the discussion into subsections.

3. HRDWARE AND SOFTWARE DESIGN

3.1 Sensor node design

The sensor node will be developed on the basis of an ARM-based STM32 microcontroller with several environmental sensors and a LoRa communication system (Table 2). The microcontroller, which will be STM32, will receive sensor data, process the measurement, and manage the communication component. Figure 2 shows that the STM32 microcontroller is the central controller of the sensor node.

Table 2. Key specifications of STM32F103C8T6 (Blue Pill or ARM Cortex-M3)

Feature	Details
Core	ARM Cortex-M3 @ 72 MHz
Flash Memory	64 KB
SRAM	20 KB
GPIOs	37 (5 V-tolerant inputs)
ADC	12-bit, 10 channels (0–3.3 V)
Timers	4x 16-bit, 2x PWM
Communication	2x I2C, 3x USART, 2x SPI, USB 2.0
Operating Voltage	2.0–3.6 V (3.3 V recommended)

Figure 2. The STM32 microcontroller

The following sensors are integrated in the monitoring system:

• DHT11 sensor for temperature and humidity measurement

DHT11 sensor has a capacitive sensor of humidity and a thermistor to check the temperature. A humidity sensor is a capacitive sensor that has two electrodes and a moist material that serves as a dielectric between the electrodes. Humidity has an influence on the capacitance value. Such variable resistance values were recorded and cause an IC to generate a digital signal.

The resistance also reduces along with the temperature as the DHT11 is able to sense temperature through an NT3C thermistor. Figure 3 demonstrates that a typical thermistor is constructed of a semiconductor polymer or a ceramic to become more sensitive to the slightest change in temperature.

Negative temperature coefficient (NTC) thermistors are used by most manufacturers of asphalt tests. The resistance varied as depicted in the graph below, and it was revealed that the working range of this resistor was between -100 ℃ and 200℃ which is reasonable to be used in the environment. The application also describes a typical non-linear response curve of an NTC thermistor, Figure 3, which is available in many applications, in temperature sensing, compensation, and control, because it is highly sensitive and responsive to thermal changes. It was used to gauge the functioning of the thermistor in different circumstances.

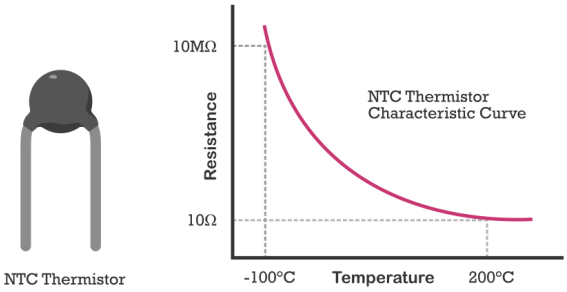

Figure 3. A negative temperature coefficient (NTC) thermistor's resistance-temperature characteristic curve

• Smoke and combustible gas detector gas sensor.

System monitoring is done with the sensor illustrated in Figure 4.

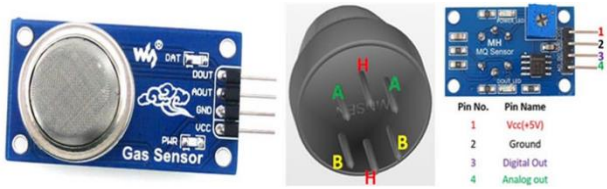

Figure 4. Gas sensors

• Photodiodes and phototransistors also require external circuitry so Light sensor monitoring illumination levels, LDRs (Figure 5) are a more viable option although they do require external circuits they can directly measure the level of light.

Figure 5. Light dependent resistor (LDR) used for light intensity measurement

The gas sensor measures the combustible gases that include LPG, methane and smoke. Thus, the measurements provided are a gas intensity index instead of actual CO_2 reading of concentration. Figure 6 is the block diagram of the sensor node.

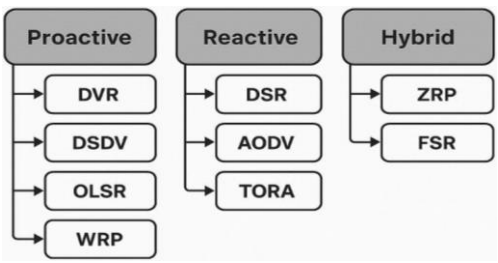

Figure 6. Block diagram of the sensor node

3.2 LoRa communication module

The LoRa communication module allows wireless communication over a long distance between sensor nodes and the gateway. LoRa technology is applicable in large scale sensor networks because of low power consumption and long-range of communication.

The LoRa communication module used in the system is shown in Figure 7.

Figure 7. The LoRa communication module

The LoRa communication parameters used in the proposed system are listed in Table 3.

Table 3. LoRa communication parameters

Parameter	Value
Frequency band	433 MHz
Bandwidth	125 kHz
Spreading factor	SF7
Coding rate	4/5
Transmit power	20 dBm
Payload size	32 bytes
Transmission interval	60 s
Network topology	Star

3.3 Gateway design

LoRa packets to sensor nodes are received by the gateway node and transmitted to a cloud server via Wi-Fi connectivity. The ESP8266 Wi-Fi module is an Internet access module. The gateway receives incoming data, and sends it to the monitoring platform in the cloud.

An example of a reactive protocol is the Ad Hoc On-Demand Distance Vector (AODV). This protocol performs better when exposed to frequent topology changes (favoring dynamic routing) because it only finds routes when there is a demand for transmission and the path to the destination is unknown or unavailable. Such a protocol enables the development of a route discovery and maintenance mechanism based on a request and response model. The route Request (RREQ), Route Reply (RREP), and Route Error (RERR) are the three primary message types used by AODV [16].

3.4 Routing protocols based on DVRs

The routers update their routing tables on a regular basis with the assistance of the dynamic, distributed, asynchronous, and iterative Distance Vector Routing Algorithm (DVRA) protocol through the information exchanged with their neighbors. All routers create a Distance Vector Table (DVT), exchange it with their neighbors, and compute the shortest path to each other in the network on a regular basis. The process goes on until a steady Distance Vector Routing Table (DVRT) is got upon which packets are sent [16].

The routers are linked by direct point-to-point connections or broadcast subnets, e.g. Ethernet or Token Ring. The route that involves minimum delay is normally called the shortest path. The routers can estimate the distances by asynchronously

transmitting time-stamped ECHO REQUEST packets and getting back the corresponding ECHO RESPONSE packets with the neighbors. DVRT is then updated by the Distributed Asynchronous Bellman-Ford algorithm. A new DVT is generated and shared among all the neighbors in case any changes are detected. To ensure successful and accurate routing, this cycle will ensure that each router is up to date with DVRT [16].

4. METHODS FOR CALIBRATION OF SENSORS

The critical examination of the approaches to the improvement of the accuracy and functionality of gas concentration sensors in particular, semiconductor-based gas sensors that are relatively cheap and prone to bias, environmental factors, and aging was done [17].

4.1 Linear function calibration

It is known as calibration when it comes to the process of removing systematic errors (biases) of sensor readings. Also, transforming the raw sensor outputs to standardized units has often been known as this term. In order to make a direct mapping of sensor outputs and required values, the customary single-sensor calibration often relies on the presentation of a specific stimulus with a known response. Therefore, the calibration of a sensor is often limited to some ranges and operating conditions, specifications of which are provided by the manufacturer of a sensor [18].

In the event that manual calibration is infeasible, the originators [19] provide an innovative procedure of calibrating thick sensor webs. Based on a temporal correlation of synchronized readings, their two-phase technique initially builds pair-wise correlations among nearby sensors.

To be precise, to achieve calibration, Figure 3 demonstrates the important difference between random noise and systematic bias.

Bias and Systematic errors: The difference between the actual xtrue and the mean value of sensor readings x is called the bias. The bias is subject to the effect of the surrounding, perceived phenomena, time, or any other factor [19].

Random Errors (Noise): The random element of this error may be due to the hardware noise, other random transient states or external interferences that influence sensor measurements. Under some circumstances, noise of measurements can be modeled by a specific distribution [19]. On the main sources of inertial sensor random errors are the two components of sensor noise, a low and a high-frequency component. The low-frequency component is characterized by correlated noise, and the high-frequency component is characterized by white noise [20].

In the event of detecting the same environmental changes (i.e., changes in temperature or changes in highlighting the gas concentration) the initial phase is that of comparing the measurements of nearby sensors. As shown in Figure 8, the two major types of inaccuracy that sensors usually exhibit are bias and noise [21]. The system uses simple linear correlations to calculate the adjustment variables between the sensor pairs. Sensor A under the same conditions uses a correction formula when it repeatedly is 5% higher than Sensor B [19]:

$$F_{\{i,j\}(x)} = a_{\{i,j\}} * x + b_{\{i,j\}}$$

Traversing a path from nodes s1 to s_2 to s_3, we have

$$F_{\{2,3\}}F_{\{1,2\}}(x) = a_{\{2,3\}} \cdot \left(a_{\{1,2\}} \cdot x + b_{\{1,2\}}\right) + b_{\{2,3\}}$$
$$= a_{\{2,3\}} \cdot a_{\{1,2\}} \cdot x + a_{\{2,3\}} \cdot b_{\{1,2\}} + b_{\{2,3\}}$$

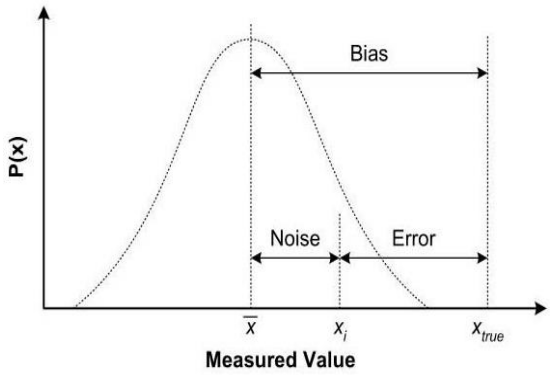

Figure 8. Sensor measurement error terminology

Two significant conclusions can be drawn from this, as stated in the study [19].

- The local scale approach to consistency should be prioritized since the calibration functions are necessarily built out of the local measurements. This implies that shorter paths should be preferred within the calibration graph (CG). This means that shorter paths are highly desired in the CG as in Figure 9 since fewer cumulative errors would be considered and local relationships would be preserved.
- It is rational to expect that there will be an increased consistency of those paths that are dominated by CFs of higher confidence due to the fact that every path in the CG is a sequence of calibration functions (CFs) of various confidence levels. It means that more confident traversals would result in more reliable and stable calibration results in a real-world application.

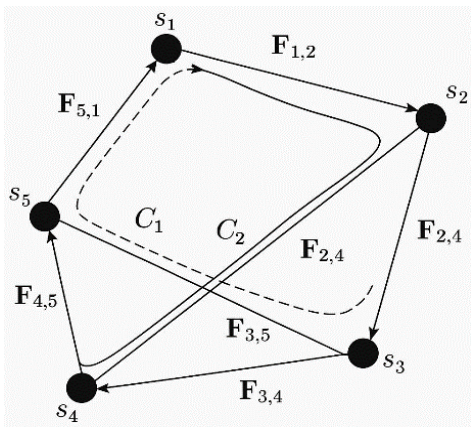

Figure 9. Sensor measurement error terminology

Nonetheless, the system will incorporate a second step of the optimization since various sensor pairs can suggest slightly different changes. This is a process that determines all the inter sensor relationships in the network as indicated in Figure 4, just as a group of experts may be able to settle their differing opinions to come up with an agreement. By analyzing these

connections, the system identifies the most reliable calibration changes to all the network. Tests in the field demonstrated that this approach was able to reduce 80% of the sensors to within 5C of the reference measurements, which is useful in real-world application where more practical accuracy is required but absolute accuracy is challenging [21, 22].

4.2 Self-calibration by combining multiple sensors

The compensation concept called cross-sensitivity compensation is one that enables both the signal to be measured X and the interfering signal C to change the signal of sensor 1. The signal C is picked up by the sensor 2 and the cross-sensitivity is eliminated by the sensor. This method requires the reproducibility of cross-sensitivity of sensor 1 to the interfering signal C. Few gains can be achieved in case there is a significant time variation in cross-sensitivity. A significant increase in the performance can be achieved by incorporating sensors, which have a specified cross-sensitivity [22, 23] as illustrated in Figure 10 to better comprehend.

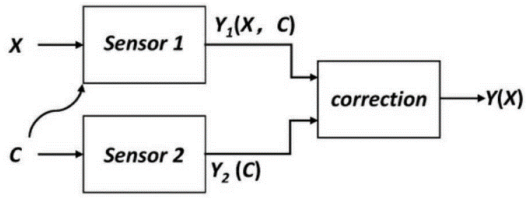

Figure 10. Compensation for cross-sensitivity

From Figure 10, we obtain the calibrated compensation:

$$Y_{corrected} = Y^1 - \left(\frac{\beta}{\gamma}\right) Y^2 \approx \alpha X + \left(\varepsilon - \left(\frac{\beta}{\gamma}\right)\delta\right)$$

where,

The calibrated compensation ratio is denoted by (β/γ).

Perfect compensation occurs when ε,δ → 0 and β/γ is stable.

A method to enhance the compensation of the two signal measures involves the use of two identical sensors to measure two signals that have the same magnitude but opposite phases (differential compensation, Figure 11(A)). These errors are removed in the next step calculation since the interfering signal C is applied to both sensors at the same time. Common differential compensation circuit is represented by Wheatstone full-bridge as shown in Figure 11(B). The strain gauges in R1, R2, R3 and R4 are shown to be orthogonal to one another [22, 23]. The changes in the four strain gauges should be the same as much as the absolute values of the changes in resistances produced by object deformation should be the same. It was simply calculated that the change in resistance was proportional to the final output voltage, Vout. The supply voltage V bias values numerically equal the sensitivity, and non-linear error is nonexistent [23].

For Figure 11(A):

$$Y(X) = Y_{1(X,C)} - Y_{2(-X,C)}$$

In Figure 11(B), the resistor ratios determine the voltage differential Vout across the bridge:

$$V_{out} = V_{bias}\left(\frac{R_4}{R_2 + R_4} - \frac{R_3}{R_2 + R_3}\right)$$

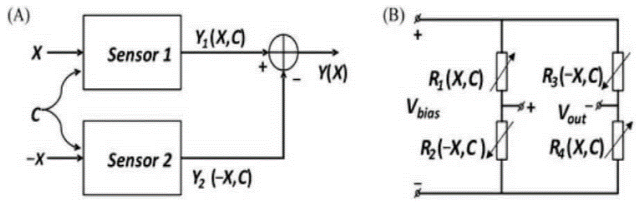

Figure 11. The application and compensation are different. (A) Compensation that is different. (B) Wheatstone Bridge

4.3 Frequency-based filtering techniques

Compared to other frequency-based filters (low-pass, high-pass or band-stop filters), Wavelet filtering is considered to be superior to conventional filters [24, 25]. The wavelet analysis is special in the sense that it can accurately focus on time windows besides filtering specific frequency components. Hence, it is especially effective with the pulsed sensors where the airflow on the sensor surface occurs periodically.

Other sensor measurement circuits employing microcontrollers to provide correction capabilities as well as thermal compensation elements to fine-tune sensor output are mentioned in the study [25].

This equation varies the ratio of resistance of the sensor to its base resistance, by applying a linear correction model:

$$\left(\frac{R_s}{R_0}\right)_{\{corr\}} = \left(\frac{R_s}{R_0}\right)(a + b * T)$$

$$\left(\frac{R_s}{R_0}\right)_{\{corr\}} = \left(\frac{R_s}{R_0}\right)(a + b * T + c * RH)$$

- ✓ *RH* is relative humidity;
- ✓ The ***c*** is a constant.

Using the corrected resistance ratio, we can estimate the gas concentration in parts per million (ppm) via a linear relation:

$$ppm = \alpha + \beta \cdot \left(\frac{R_s}{R_0}\right)_{\{corr\}}$$

These models are used to refine the sensor's output to better reflect actual gas concentrations.

Linear and Nonlinear Function Models:

1. **Linear 1st-order model**:

$$y = b_0 + b_1x_1 + b_2x_2 + b_3x_3$$

2. **Quadratic with interaction terms**:

$$y = y_0 + b_1x_1 + b_2x_2 + b_3x_3 + b_{\{12\}x_1x_2} + b_{\{13\}x_1x_3} + b_{\{23\}x_2x_3}$$

3. **Polynomial with squared terms**:

$$y = b_0 + b_1x_1 + b_2x_2 + b_3x_3 + b_{\{11\}x_1^2} + b_{\{22\}x_2^2} + b_{\{33\}x_3^2}$$

4. **Comprehensive non-linear model (including squares and interactions)**:

$$y = b_0 + b_1x_1 + b_2x_2 + b_3x_3 + b_{\{11\}x_1^2} + b_{\{22\}x_2^2} + b_{\{33\}x_3^2} + b_{\{12\}x_1x_2} + b_{\{13\}x_1x_3} + b_{\{23\}x_2x_3}$$

where,

- ✓ x_1: voltage across the sensor,
- ✓ x_2: load resistance,
- ✓ x_3: temperature.

4.4 Piecewise linear approximation

The PLA family of linear approximation methods is a representation of data samples with a series of line segments but with the original samples also present within an approximation error tolerance. The PLA method aims to reduce the amount of energy consumed during the transmission of data by using a line sequence to approximate the time series; the endpoints of all lines are only two. This hypothesis is confirmed by Figure 7 with the help of the same data. PLA leads to an effective time series representation in respect to memory and transmission needs since a line section can be determined utilizing merely two source points [26].

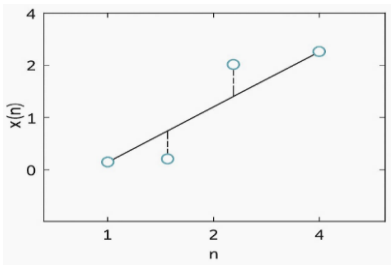

Figure 12. Approximation of a time series x(n) by a segment

4.5 Receiver-side signal approximation

The original signal samples are approximated at the receiver end by vertically projecting the signal samples on their respective line segments, as shown in Figure 12. The output of this value, which is denoted as, is the estimated signal. The disparity between the original sample and the projected approximation is the approximation error, and is determined by the following expression [26]:

The technique will assist in simplifying the received information but at the same time give a close representation of the original signal.

5. EXPERIMENTAL RESULTS AND DISCUSSION

The monitoring system proposed was tested in a laboratory set up to measure the functionality of the monitoring of wireless communication and environment.

Figures 13 and 14 demonstrate the physical prototype of the created monitoring system.

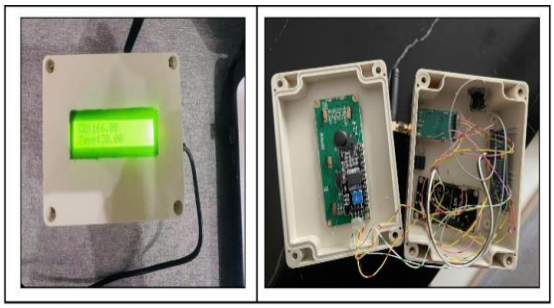

Figure 13. Model and location of system devices for the master node, showing the measured value results

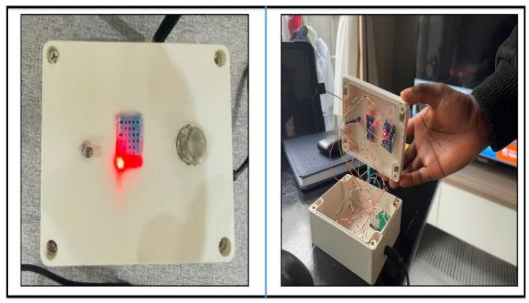

Figure 14. Model and location of system devices for the slave node

5.1 Environmental data monitoring

The sensor nodes were used to gather continuous environmental data of temperature, humidity, intensity of gases and light. Table 4 shows some of the sample temperatures taken as part of the experiment.

Table 4. Temperature measurement results

Time	Reference Temperature (℃)	Measured Temperature (℃)	Absolute Error (℃)
08:00	26.8	27.1	0.3
09:00	27.0	27.3	0.3
10:00	27.5	27.9	0.4
11:00	28.1	28.4	0.3

The absolute error was calculated using:

Absolute Error = Measured value -Reference value.

The findings indicate that sensor measurements are highly consistent with the reference measurements with a low level of deviation.

After showing the physical devices, we proceed to the results of the application interface and its visualization. The comparison of the actual temperature values with the values the device recorded reveals that within the result tables provided of all three days, the system worked within a comfortable range of error. Figure 15 shows the process of organizing and storing the received data in the IoT Firebase cloud database.

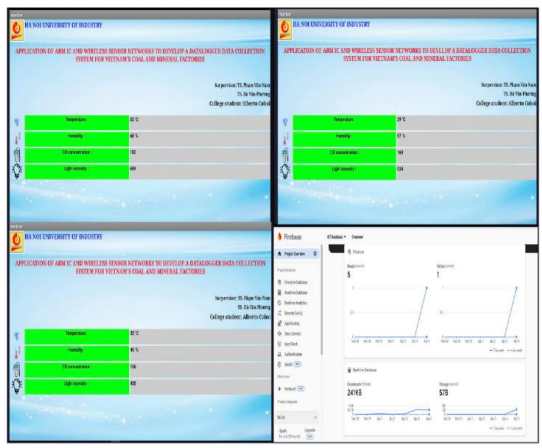

Figure 15. Environmental monitoring data stored in Firebase cloud platform

A summary of the obtained data during three days at different time of day is given in Tables 5, 6, and 7. The data

obtained showed that the temperature level generally changed depending on time of day. The error margin of the measurement was varying with the environmental conditions and sensor sensitivity.

Table 5. Day 1 results

Time	Actual Temp (°C)	Measured Temp (°C)	Absolute Error (°C)	Relative Error (%)	Humidity (%)	CO (ppm)	Light (lux)
09:00 AM	7.0	27.3	0.3	1.11%	60	5	300
12:00 PM	30.5	31.0	0.5	1.64%	58	6	520
03:00 PM	32.0	32.5	0.5	1.56%	57	5	480
06:00 PM	28.0	28.1	0.1	0.36%	61	4	120

Table 6. Day 2 results

Time	Actual Temp (°C)	Measured Temp (°C)	Absolute Error (°C)	Relative Error (%)	Humidity (%)	CO (ppm)	Light (lux)
09:00 AM	26.5	26.8	0.3	1.13%	62	5	310
12:00 PM	31.0	31.4	0.4	1.29%	59	7	540
03:00 PM	33.0	33.6	0.6	1.82%	56	6	500
06:00 PM	28.5	28.3	0.2	0.70%	60	5	130

Table 7. Day 3 results

Time	Actual Temp (°C)	Measured Temp (°C)	Absolute Error (°C)	Relative Error (%)	Humidity (%)	CO (ppm)	Light (lux)
09:00 AM	27.5	27.9	0.4	1.45%	63	4	320
12:00 PM	32.0	32.7	0.7	2.19%	58	6	560
03:00 PM	34.0	34.5	0.5	1.47%	57	6	510
06:00 PM	29.0	28.7	0.3	1.03%	62	5	150

The initial one was to graphically depict the tendencies in the given parameters of the environment, i.e., temperature, CO concentration, light intensity, and humidity. Data were collected within 3 days in intervals of 4 hours: 9:00 AM, 12:00 PM, 03:00 PM, and 6:00 PM. On day 2, CO levels were observed to increase to around 7ppm at about 12:00 PM. This is an indicator of processes occurring in the day or an alteration of the environment that is brought about by the day time cycles of temperature and light. This trend information allows easier identification of trends and give a reasonably good picture of the environmental behavior on a longer time scale. This study can be useful to environmental conscious decision-making systems.

5.2 Wireless communication performance

The performance of the LoRa network in terms of communication was determined by measuring the received signal strength indicator (RSSI) at varying distances, as shown in Table 8. The findings show that the LoRa communication connection has a steady long-range connectivity.

5.3 Power consumption analysis

Energy efficiency of the sensor node was measured by measuring power consumption.

The experimental values of the current consumption were:

Sleep mode: 2 mA

Sensing mode: 18 mA

LoRa transmission: 120 mA

Due to a 2000 mAh battery, a transmission rate of 60 seconds, the sensor node is expected to have a lifespan of about 6 to 8 months.

Table 8. Received signal strength indicator (RSSI) measurements

Distance	RSSI
100 m	−85 dBm
300 m	−92 dBm
500 m	−102 dBm

5.4 Packet delivery ratio

The dependability of the wireless communication link was tested through the packet delivery ratio (PDR). PDR gives the percentage of packets received successfully to the number of packets sent. Table 9 shows the packet delivery performance of the system.

$$PDR = \frac{Received\ Packets}{Transmitted\ Packets} \times 100$$

Table 9. Packet delivery performance of the system

Test Environment	Transmitted Packets	Received Packets	PDR
Indoor	100	96	96%
Outdoor	100	98	98%

The findings show that the monitoring system is based on a LoRa-based monitoring system that has reliable communication performance.

5.5 Network latency analysis

Network latency is the duration which sensor data takes to pass through sensor node to the gateway.

Table 10 shows the measured latency values during the experiments.

Table 10. Measured latency values

Distance	Average Latency
100 m	180 ms
300 m	210 ms
500 m	240 ms

The findings reveal that the system offers tolerable latency in the application of environmental monitoring.

5.6 System testing

Once this was done, the trends of the given environmental parameters (Figure 16), i.e., temperature, CO concentration, light intensity and humidity, were visualized. Three days of data were collected at an interval of 4 hours 9:00 AM, 12:00 PM, 03:00 PM, and 6:00 PM. On Day 2, the CO concentration increased to about 7ppm at about 12:00 pm. This is an indication of operations that occur in the day or variations in the environment due to the daytime variations on the temperature and light intensities. Patterns identified through such trend data are simpler to detect, and might give an adequate summary of the behaviour of the environment over a longer time period. This study can be useful to environmentally conscious decision-making systems.

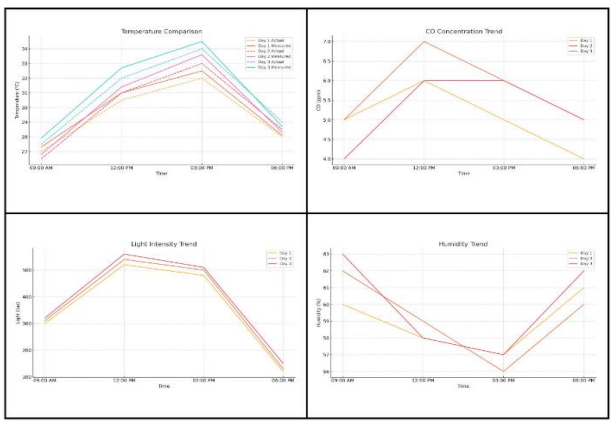

Figure 16. The four quadrants show the daily trend summaries of environmental variables

6. CONCLUSION

This paper introduced a design and implementation of a wireless sensor network to monitor the environment at the mines using ARM based sensor network. The suggested system incorporates several environmental sensors and the LoRa communication technology to provide the capability of transmitting wireless data at long distances. The software architecture comprises of distributed sensor nodes, LoRa gateway, and a monitoring platform on the cloud.

As can be seen through the experimental results, the proposed monitoring system offers quality data acquisition on the environmental conditions and stable wireless communication. LoRa communication allows long-range communication with low power consumption, and therefore, the system is applicable to large-scale use in mining environments.

The next step of work will be performed in order to enhance the scalability of the system, to incorporate more environmental sensors and to provide more sophisticated data analytics to predictive monitoring in mining setting.

REFERENCES

[1] Nguyen, Q.N., Nguyen, V.H., Pham, T.P., Chu, T.K.L. (2021). Current status of coal mining and some highlights in the 2030 development plan of coal industry in Vietnam. Inżynieria Mineralna, 1(2): 373-380. http://doi.org/10.29227/IM-2021-02-34

[2] Bui, N.X., Nguyen, H., Lee, C., Le, T.Q., Van Bui, T. (2021). Effects of meteorological conditions on the air quality in deep open-pit mines in Vietnam. Journal of Mining and Earth Sciences, 62(4): 1-14. http://doi.org/10.46326/JMES.2021.62(4).01

[3] Mahdevari, S., Shahriar, K., Esfahanipour, A. (2014). Human health and safety risks management in underground coal mines using fuzzy TOPSIS. Science of the Total Environment, 488: 85-99. https://doi.org/10.1016/j.scitotenv.2014.04.076

[4] Zvarivadza, T., Onifade, M., Dayo-Olupona, O., Said, K.O., Githiria, J.M., Genc, B., Celik, T. (2024). On the impact of Industrial Internet of Things (IIoT)-mining sector perspectives. International Journal of Mining, Reclamation and Environment, 38(10): 771-809. https://doi.org/10.1080/17480930.2024.2347131

[5] Chavan, S.V., Tilekar, S.K., Mane-Deshmukh, P.V., Ladgaonkar, B.P. (2017). ARM microcontroller based wireless sensor network to monitor environmental parameters of textile industry. International Journal of Advanced Research in Computer Science and Software Engineering, 7(5): 438-449.

[6] Silva, J.D.C., Rodrigues, J.J., Alberti, A.M., Solic, P., Aquino, A.L. (2017). LoRaWAN—A low power WAN protocol for Internet of Things: A review and opportunities. In 2017 2nd International Multidisciplinary Conference on Computer and Energy Science (SpliTech), pp. 1-6.

[7] Da Xu, L., He, W., Li, S. (2014). Internet of things in industries: A survey. IEEE Transactions on industrial informatics, 10(4): 2233-2243. https://doi.org/10.1109/TII.2014.2300753

[8] Mousavi, S.M., Khademzadeh, A., Rahmani, A.M. (2022). The role of low-power wide-area network

technologies in the Internet of Things: A systematic and comprehensive review. International Journal of Communication Systems, 35(3): e5036. https://doi.org/10.1002/dac.5036
[9] Ohwo, O.B., Olujimi, A.D. (2020). A comparative review of emerging wireless technology. International Journal of Scientific Research in Computer Science, Engineering and Information Technology, 7: 163-175. https://doi.org/10.32628/CSEIT206536
[10] Nguyen, Q.K. (2024). How does financial flexibility strategy impact on risk management effectiveness? Sage Open, 14(2): 21582440241240842. https://doi.org/10.1177/21582440241240842
[11] Lee, H.C., Ke, K.H. (2018). Monitoring of large-area IoT sensors using a LoRa wireless mesh network system: Design and evaluation. IEEE Transactions on Instrumentation and Measurement, 67(9): 2177-2187. https://doi.org/10.1109/TIM.2018.2814082
[12] Reddy, G.P., Kumar, Y.P. (2021). Demystifying LoRa wireless technology for IoT applications: Concept to experiment. In 2021 4th International Symposium on Advanced Electrical and Communication Technologies (ISAECT), Alkhobar, Saudi Arabia, pp. 1-6. https://doi.org/10.1109/ISAECT53699.2021.9668500
[13] Chowdhury, A.R., Lee, T.A., Day, C., Hutter, T. (2022). A review of preconcentrator materials, flow regimes and detection technologies for gas adsorption and sensing. Advanced Materials Interfaces, 9(20): 2200632. https://doi.org/10.1002/admi.202200632
[14] Yadav, V., Thakur, M. (2021). Environmental risk monitoring assessment and management. In Basic Concepts in Environmental Biotechnology, pp. 213-222.
[15] Sundaram, J.P.S., Du, W., Zhao, Z. (2019). A survey on LoRa networking: Research problems, current solutions, and open issues. IEEE Communications Surveys & Tutorials, 22(1): 371-388. https://doi.org/10.1109/COMST.2019.2949598
[16] Debbarma, M.K., Debbarma, J., Sen, S.K., Roy, S. (2013). Dvr-based hybrid routing protocols in mobile Ad-hoc network: Application and challenges. IJRET: International Journal of Research in Engineering and Technology, 2(2): 9-13.
[17] Nikolic, M.V., Milovanovic, V., Vasiljevic, Z.Z., Stamenkovic, Z. (2020). Semiconductor gas sensors: Materials, technology, design, and application. Sensors, 20(22): 6694. https://doi.org/10.3390/s20226694
[18] Xiong, X., Cao, C., Chander, G. (2010). An overview of sensor calibration inter-comparison and applications. Frontiers of Earth Science in China, 4(2): 237-252. https://doi.org/10.1007/s11707-010-0002-z
[19] Bychkovskiy, V., Megerian, S., Estrin, D., Potkonjak, M. (2003). A collaborative approach to in-situ sensor calibration. In Information Processing in Sensor Networks, pp. 301-316.
[20] El-Diasty, M., Pagiatakis, S. (2008). Calibration and stochastic modelling of inertial navigation sensor errors. Journal of Global Positioning Systems, 7(2): 170-182.
[21] Ren, B., Jia, T., Liu, H., Wang, Y., Yan, J. (2024). Efficient estimation for sensor biases and target states in the presence of sensor position errors. IEEE Sensors Journal, 24(10): 16551-16562. https://doi.org/10.1109/JSEN.2024.3384810
[22] Delaine, F., Lebental, B., Rivano, H. (2020). Framework for the simulation of sensor networks aimed at evaluating in situ calibration algorithms. Sensors, 20(16): 4577. https://doi.org/10.3390/s20164577
[23] Barcelo-Ordinas, J.M., Doudou, M., Garcia-Vidal, J., Badache, N. (2019). Self-calibration methods for uncontrolled environments in sensor networks: A reference survey. Ad Hoc Networks, 88: 142-159. https://doi.org/10.1016/j.adhoc.2019.01.008
[24] Fu, J., Gao, Q., Li, S. (2023). Application of intelligent medical sensing technology. Biosensors, 13(8): 812. https://doi.org/10.3390/bios13080812
[25] Nakamoto, T., Ikeda, T., Hirano, H., Arimoto, T. (2009). Humidity compensation by neural network for bad-smell sensing system using gas detector tube and built-in camera. In SENSORS, 2009 IEEE, Christchurch, New Zealand, pp. 281-286. https://doi.org/10.1109/ICSENS.2009.5398164
[26] Zuppa, M., Distante, C., Persaud, K.C., Siciliano, P. (2007). Recovery of drifting sensor responses by means of DWT analysis. Sensors and Actuators B: Chemical, 120(2): 411-416. https://doi.org/10.1016/j.snb.2006.02.049